Gonzalez-Chomon, C.; Haramus, V.M.; Rangelov, S.; Ebdon, J.R.; Novakov, C.; Halacheva, S.S.:
Trimethoxysilyl end-capped hyperbranched polyglycidol/polycaprolactone copolymers for cell delivery and tissue repair: synthesis, characterisation and aqueous solution properties.
In: European Polymer Journal. Vol. 112 (2019) 648 - 659.
First published online by Elsevier: 22.10.2018

DOI: /10.1016/j.eurpolymj.2018.10.030
https://dx.doi.org/10.1016/j.eurpolymj.2018.10.030

Trimethoxysilyl End-capped Hyperbranched Polyglycidol/Polycaprolactone Copolymers for Cell Delivery and Tissue Repair: Synthesis, Characterisation and Aqueous Solution Properties

Clara González-Chomón[a], Vasil M. Garamus[b], Stanislav Rangelov[c], John R. Ebdon[a], Christo Novakov[c] and Silvia S. Halacheva[a*]

[a] University of Bolton, Deane Road, Bolton, Greater Manchester, BL3 5AB, U.K.

[b] Abt. WBM, Bldg. 47, R. 317, Helmholtz-Zentrum Geesthacht, Zentrum für Material- und Küstenforschung GmbH, Max-Planck-Str., 21502 Geesthacht, Germany

[c] Institute of Polymers, Bulgarian Academy of Sciences, Acad. G. Bonchev, Bl. 103A, Sofia, Bulgaria

Abstract

New PCL-HBPG/SiHBPG triblock copolymers composed of a polycaprolactone (PCL) core with two outer blocks of trimethoxysilyl end-capped hyperbranched polyglycidol (HBPG/SiHBPG), of varying molecular weight, have been successfully synthesised and characterised. The effect of copolymer composition and structure upon the crystallization, melting, thermal degradation and aqueous solution behaviour were investigated at various temperatures. In aqueous solution, at concentrations above their corresponding critical aggregation concentration the PCL-HBPG/SiHBPG copolymers readily self-assemble into large multicore structures composed of PCL domains and corona consisting of HBPG/SiHBPG branches. The multicore structures were stabilized by numerous hydrogen-bonds from the HBPG moieties as well as via formation of siloxane crosslinks (i.e. Si–O–Si bonds). As the siloxane linkages are irreversible the PCL-

HBPG/SiHBPG-based particles will be covalently crosslinked at higher concentrations *in vivo* and form injectable gels scaffolds that will be biocompatible and capable of invoking cell attachment and differentiation without the need for exogenous biological stimuli.

Introduction

In reconstructive medicine there is a tremendous need for suitable biomaterials to allow the repair and regeneration of damaged or diseased tissue.[1] A large range of injectable gel scaffolds have been investigated, developed and subsequently applied in tissue engineering because their structure and properties can be easily varied and eventually optimised.[2] The injectable scaffolds intended for use in regenerative medicine should be (i) biocompatible; (ii) injectable, the scaffold formulation should be sufficiently fluid and not undergo premature solidification; (iii) biodegradable, the scaffold should degrade at a rate comparable to that of new tissue regeneration and (iv) of sufficient mechanical strength and tissue adhesivness. Although a large amount of work has been carried out in this area, injectable scaffolds/cell suspensions are still not used clinically. The scaffold design parameters must be fully optimised and controlled before such scaffolds can become a clinical reality.

Linear aliphatic polyesters such as poly(ε-caprolactone) (PCL), polylactide (PLA) and polyglycolide (PGA) have recently attracted attention in biomaterials science because of their biodegradability and biocompatibility.[3, 4] Notably, PCL has been approved by the FDA for use as a surgical suture. However, the hydrophobic and semicrystalline nature of PCL, as well as the absence of utilisable functional groups on the polymer backbone, have limited its practical applications.[4] A wide variety of PCL-based biomaterials that exhibit desirable properties have been developed by appropriate selection of co-monomers to be polymerised with ε-

caprolactone.[5] For example, injectable, porous thermo-responsive scaffolds based on poly(ethylene glycol)-block-poly(ε-caprolactone) (PEG-b-PCL-b-PEG)[6] and hyperbranched polycaprolactone-click-poly(*N*-vinylcaprolactam) (HBPCL-click-VPCL)[7] have been used for tissue regeneration. The scaffolds were able to support the proliferation and differentiation of the embedded cells and promote tissue growth. Despite such encouraging results, there are still many challenges that need to be overcome in the future, in order that the PCL-based biomaterials be successfully utilised in reconstruction medicine.[8]

Hydrophilic hyperbranched polyglycidol (HBPG) polymers have emerged as a new promising platform in tissue engineering applications because of their strong biocompatibility,[9] desirable mechanical properties, high transport capacity, and multiple pendant hydroxyl-groups which can be used as attachment sites for targeting biological cells and tissues.[10, 11] In addition, oligoglycidols are approved as food and pharmaceutical additives by the FDA. Recently, the chemical modification of the surface of biomaterials with methyl and hydroxyl functional groups has shown promise in enhancing the ability of a material to support mesenchymal stem cell (MSC) adhesion and differentiation.[12] We propose that the presence of numerous hydroxyl groups in HBPG will be therefore able to promote the cellular attachment and differentiation without exogenous biological stimuli.

Diblock copolymers based on linear PEG and HBPG were previously synthesised by Wilms et al.[13] using a two-step procedure. A multistep approach, utilising DL-1,2-isopropylidene glyceryl glycidyl ether as a monomer followed by deprotection to unmask the hydroxyl groups, has been also adopted by Wurm et al.[14] for the synthesis of triblock copolymers based on PEG and HBPG. Halacheva et al.[15, 16] have prepared a range of thermo-responsive linear polyglycidol-block-poly(propylene oxide)-block-linear polyglycidol (PG-b-PPO-b-PG) physical

gel networks through ordered packing of bridged copolymer micelles. The mechanical properties and stability of the gels were tuneable by varying the copolymer composition. Densely and loosely grafted PG-g-PCL copolymers were synthesised by ring-opening polymerisation of ε-caprolactone using linear or star-shaped PG as a macroinitiator.[17] Multiarm star HBPG-b-PCL block copolymers were prepared using either tin(II)- or aluminium-based catalysts, which limits the potential application of the copolymers *in vivo*.[18, 19] Xu et al.[20] synthesised statistical poly(ε-caprolactone-co-tert-butyl glycidyl ether) copolymers utilizing 1-tert-butyl-4,4,4-tris(dimethylamino)-2,2-bis[tris(dimethylamino)phosphoranylidenamino]-2Λ5,4Λ5. The crystallization properties, enzymatic degradation, and cytotoxicity of the copolymers were evaluated as a function of copolymer composition. Cai et al.[21] synthesized surface-functionalizable membranes of PCL-click-HBPG by a combination of ring-opening polymerization of glycidol, atom transfer radical polymerization and click chemistry. The pore size and porosity of the membrane were controlled by varying the HBPG content. Recently, Kim et al.[22] investigated the potential application of well-defined photocrosslinkable amphiphilic PCL-b-HBPG-based block copolymers for drug delivery. The copolymers were synthesised via anionic polymerization of glycidol using partially deprotonated linear PG-b-PCL copolymers as macroinitiators. The copolymers exhibited improved biocompatibility and stability and supported the sustained release of ibuprofen *in vitro*. Herein we adopt and optimise this approach in order to synthesise a series of novel ABA triblock copolymers which are composed of a middle block of hydrophobic PCL and outer moieties of hydrophilic HBPG and trimethoxysilyl HBPG (SiHBPG). The new trimethoxysilyl-capped PCL-HBPG copolymers (PCL-HBPG/SiHBPG) are synthesised by anionic polymerization of glycidol and (3-glycidyloxypropyl)trimethoxysilane. The PCL-HBPG/SiHBPG copolymers will be further

utilized for development of injectable PCL-HBPG/SiHBPG-based gels which can be covalently crosslinked *in vivo* due to the gradual hydrolysis of trimethoxysilyl groups. Hydrolysable silanes are commonly used as coupling agents due to their facile hydrolysis and subsequent siloxane (Si–O–Si) crosslink formation. [23, 24] In aqueous media the trimethoxysilyl groups readily hydrolysed and created silanol moieties that subsequently condensed, crosslinking the material. Therefore, we propose that the physical network of the PCL-HBPG/SiHBPG particles will be locked in place *in vivo* to generate covalently-linked gels that exhibit gradually increasing mechanical strength over time.

To control the process of gel formation and develop an injectable scaffold formulation that is sufficiently fluid and does not undergo premature solidification it is essential that we first investigate the aqueous solution behaviour of the PCL-HBPG/SiHBPG copolymers and correlate the results with the polymers' structures, composition and supramolecular level interactions. The results of the investigation will add new knowledge to the structure property relationships of the PCL-HBPG/SiHBPG based formulations and will give valuable hints for further fine-tuning of these systems. To the best of our knowledge no data have been reported so far regarding the synthesis, characterisation, thermal behaviour and aqueous solution properties of PCL-HBPG/SiHBPG-based biomaterials. In the present contribution the aqueous solution behaviour of the PCL-HBPG/SiHBPG copolymers is investigated over wide temperature and concentration ranges by dye solubilization, turbidimetry, light scattering and small angle X-ray scattering, aiming to provide valuable structural insights and elucidating the properties of the self-assembled structures and, eventually, the injectable gels thereof.

Experimental Section

A. Materials. Toluene (Acros, >99%), diethyl ether (Acros, >99.5%), methanol (Acros, 99.9%), glycidol (Acros, 96%), poly(ε-caprolactone) (Acros, 99%, average molecular weight 2000 g/mol), sodium methoxide (Acros, 30 wt% solution in methanol), (3-glycidyloxypropyl)trimethoxysilane (Sigma Aldrich, ≥98%), diatomaceous earth, acid-washed (MP Biomedicals, 95%), 1,6-diphenyl-1,3,5-hexatriene (DPH, Sigma Aldrich, 98%) and DMSO-d_6 were used as received.

B. Synthesis of the copolymers. The copolymer abbreviations used here identify the percentage content of PCL, HBPG and SiHBPG. For example, PCL-73HBPG/1SiHBPG contains 73 mol% HBPG, 1 mol% SiHBPG and 26 mol% PCL units. The following synthesis of PCL-73HBPG/1SiHBPG is representative of the procedures employed for the other copolymers. To prepare the macroinitiator a three-neck flask, fitted with a distillation adapter, was charged with PCL diol (4.50 g, MW 2000 g/mol, 2.5 mmol), sodium methoxide (30 wt% solution in methanol, 0.31 ml, 0.29 g NaOMe, 1.35 mmol) and anhydrous toluene (50 ml), under a flow of nitrogen. The magnetically stirred solution was heated to 50 °C under reduced pressure (10 mbar approx.) and 20 ml of distillate was collected in order to remove methanol and complete the deprotonation step. Maintaining the temperature of 50 °C, a mixture of glycidol (10.41 g) and (3-glycidyloxypropyl)trimethoxysilane (0.337 g) was introduced to the solution at a uniform rate over a period of five hours. After the feed the reaction was allowed to proceed at 50 °C for 48 hours. The reaction was terminated by the addition of methanol (5 ml) at room temperature. The sample was filtered through celite, rinsing through with fresh methanol (2 × 20 ml). The filtrate was concentrated under reduced pressure to a volume of approximately 20 ml and then poured into 200 ml of cold diethyl ether. The precipitated copolymer was dissolved in 5 ml of methanol, transferred to a smaller flask and the solvent evaporated under reduced pressure. Traces of

methanol were removed under high vacuum. The molar ratios of PCL to HBPG and SiHBPG to HBPG in the copolymer were determined by ^{1}H NMR spectroscopic analysis. The silicon content in the copolymer was determined by thermogravimetric analysis (TGA). The other copolymers were obtained in an analogous manner from appropriate mixtures of HBPG and SiHBPG, with PCL.

C. Methods. *^{1}H NMR spectra* were recorded at 250 MHz on a Bruker WM 250 spectrometer. The samples were prepared as solutions in DMSO-d_6. The chemical shifts are given in ppm relative to tetramethylsilane.

Gel permeation chromatography (GPC) analyses were carried out with an Alliance Waters e2695 Separations Module equipped with an Optilab T-rEX refractive index detector (Wyatt Techn.). Chromatographic separation was achieved by a set of two Waters Ultrahydrogel GPC columns with nominal pore sizes of 120 and 1000 Å. Aqueous 0.1 M $NaNO_3$-methanol (10 %) solution was used as an eluent at a flow rate of 0.8 ml/min at 35 °C. Samples were prepared as solutions in H_2O/MeOH mixtures. Polyethylene glycol standards were used for calibration. The data was collected through Waters e-SAT/IN digital to analogue converter and molecular mass characteristics were calculated with the help of Empower 3 software (Waters Corp.).

Fourier transform, infrared (FTIR) spectroscopy analyses of the copolymers were carried out on a Thermo Scientific IS10 Nicolet FTIR spectrometer coupled with the smart iTR accessory. Absorbance IR spectra of the samples were collected over the frequency range 700 to 4000 cm^{-1}.

Differential scanning calorimetry (DSC) was conducted on a TA Instruments DSC Q2000 (coupled to a refrigerated cooling system 90; 4 – 6 mg sample size) under a nitrogen flow of 50 ml/min. Samples were cooled to −80 °C at a rate of 10 °C/min and held for three minutes. Then, samples were heated to 250 °C at the same rate and an isothermal of three minutes was applied.

This first cycle was used to remove any previous thermal history and the same cooling and heating processes were repeated in a second cycle, where the glass transition temperature (T_g) was taken to be the centre of the inflexion in the heat flow *vs*. temperature curve associated with the transition. The melting temperature (T_m) was taken as that corresponding to the maximum (peak) heat flow in the re-heating process (second heating).

The turbidity was determined by measuring the transmittance at 500 nm of aqueous solutions of the copolymers with concentrations ranging from 1 to 5 mg/ml at various temperatures using a Camspec Model M550 Double Beam Scanning UV/Visible Spectrophotometer (¼ VGA Display, 190-1100 nm, 1.8 nm bandpass). The samples were placed in a thermostated cuvette holder and heated slowly with a heating rate of 3 °C/min from ca. 5 to 80 °C.

Dye solubilisation was employed for determination of the critical aggregation concentrations (CACs). Aqueous solutions (2.0 ml) of a given copolymer in the concentration range from 0.001 – 10 mg/ml were prepared at room temperature. 1,6-Diphenyl-1,3,5-hexatriene (DPH, 10 µl of 4 mM solution in methanol) was added to each of the copolymer solutions. The solutions were incubated in the dark for 16 hours at room temperature. The absorbance in the wavelength interval 340 – 500 nm was followed at temperatures ranging from 25 to 60 °C on a UV-*vis* spectrophotometer. The main absorption peak, characteristic for DPH solubilized in a hydrophobic environment, was at 356 nm.

Static Light Scattering (SLS). Information on the weight-average molar masses, M_w, the radii of gyration, R_g, and the second virial coefficients, A_2, for the particles formed in the dilute aqueous solutions of PCL-HBPG/SiHBPG copolymers, was obtained from the SLS data using DAWN HELEOS-II multi-angled laser light scattering (MALLS) detector (Wyatt Techn.) operating at 633 nm wavelength applying the Zimm plot method. The angular dependence of the reduced

scattered light intensity, Kc/R_θ, of the copolymer solutions was measured in the experiments. Here $K = 4\pi^2 n^2 (dn/dc)^2 / N_A \lambda^4$, where N_A is Avogadro's constant and λ is the wavelength of the light in a vacuum. The refractive index increment, *dn*/*dc*, was measured using an Optilab T-rEX DRI (Wyatt Techn.) differential refractometer operating at the same wavelength as the MALLS detector. For the present systems *dn/dc* of 0.12 ml/g was obtained and used in calculations of the static parameters. R_θ is the Rayleigh ratio at a given angle (θ). The reduced scattered light intensity was either linearly dependent on $sin^2(\theta/2)$ or slightly curved, indicating that the chosen angle range was appropriate.

The *small-angle X-ray scattering* (SAXS) experiments were performed with a laboratory SAXS instrument (Nanostar, Bruker AXS GmbH, Karlsruhe, Germany). The instrument includes an IμS micro-focus X-ray source with a power of 30 W using the wavelength of the Cu Kα line. As the detector, a VÅNTEC-2000 detector (14 × 14 cm^2 and 2048 × 2048 pixels) was used. The sample to detector distance was 108.3 cm and the accessible *q* range was from 0.01 – 0.23 $Å^{-1}$. Samples were filled into glass capillaries of 2 mm diameter with temperature control (ΔT = 0.1 K). The raw scattering data were corrected for the background from the solvent measured in a capillary with the same diameter and then converted to absolute units using the scattering of pure water measured at 20 °C.

Results and discussion

Synthesis and characterisation of the HBPG/SiHBPG and PCL-HBPG/SiHBPG copolymers.

To synthesise the HBPG/SiHBPG copolymer, an anionic polymerization of a mixture of glycidol and (3-glycidyloxypropyl)trimethoxysilane initiated by 2-ethyl-2-(hydroxymethyl)-1,3-propanediol was employed. In this reaction nominally 10% of the hydroxyl groups of the inititiator were converted into the alkoxide. The method is similar to those used previously for

the synthesis of analogous HBPG polymers.[19, 25, 26] The PCL-HBPG/SiHBPG copolymers were also synthesised by anionic polymerization of a mixture of glycidol and (3-glycidyloxypropyl)trimethoxysilane but using partially deprotonated PCL diol with molecular weight of 2000 g/mol as a macroinitiator. The reaction is shown in Scheme 1. Our approach is similar to that previously described by Liang et al.[27] for the synthesis of biocompatible star-like PCL-HBPG copolymers. Walach et al.[28] has previously reported that the one-step approach for the synthesis of HBPG-b-PEG-b-HBPG copolymers employing deprotonated PEG as a macroinitiator resulted in the formation of a mixture of homo-HBPG and the desired HBPG-b-PEG-b-HBPG. The homopolymerization was attributed to the dominating contribution of the chain transfer reaction to the hydroxyl group of glycidol compared to the chain propagation. To minimize chain transfer reactions, a slow monomer addition strategy has been employed, which is based on rapid exchange equilibrium between active and dormant chain ends that leads to deactivation of active sites after a few propagation steps.[29] This approach is similar to the ring-opening, multi branching polymerization (ROMBP) strategy that has been previously utilised for the synthesis of some other hyperbranched aliphatic polyethers with controlled molecular weights and narrow molecular weight distribution; it has been shown that slow monomer addition minimizes both the homopolymerization of glycidol and the cyclization.[19] To control the concentration of alkoxides in the polymerization and thus the simultaneous growth of all chain ends, we have converted up to 30% of the hydroxyl groups into the alkoxide using sodium methoxide followed by removal of methanol. A similar approach has been previously adopted for the synthesis of well-characterised triblock copolymers of PPO and PG.[15, 16] Partially deprotonated macroinitiators were also employed to obtain star-like PCL-HBPG-based

copolymers,[27] linear-hyperbranched amphiphilic PS-b-(PB-b-PG)[30] and PEO-HBPG-based copolymers.[31]

We carried out a number of polymerizations to prepare PCL-HBPG/SiHBPG copolymers with HBPG and SiHBPG contents varying from 45 to 90 mol% and from 0.6 to 1.4 mol%, respectively. The weight average molecular weights (M_w) and dispersity indices (M_w/M_n) of the copolymers were determined by GPC. The copolymers had M_w ranging from 1,200 to 25,000 g/mol (Table 1). GPC analyses gave monomodal or bimodal distributions (Fig. 1S, ESI) with dispersity indices of the low and high molecular weight fractions ranging from 1.13 to 1.82 and from 1.13 to 1.30, respectively (Table 1). For the copolymers with bimodal distribution the low molecular weight fractions corresponded to the main products, whereas the high molecular weight fraction was likely due to the formation of condensates as a result of premature hydrolysis of trimethoxysilyl groups in SiHBPG units of the copolymers and subsequent Si–O–Si crosslink formation. However, the fraction of condensates was much smaller (see Table 1) than that of the main products and therefore would not affect the properties of the systems, i.e. thermal and aqueous solution behaviour. It can be seen from Table 1 that the measured M_w for the copolymers were lower than the theoretical values. This disparity is a consequence of an inability to properly calibrate the GPC for these polymer systems. Undoubtedly in the H_2O/MeOH solvent used for the GPC the PCL segments are tightly coiled. This, coupled with the fact that HBPG segments are hyperbranched and therefore occupy a low hydrodynamic volume, means that the GPC measurements of M_w will be underestimated.

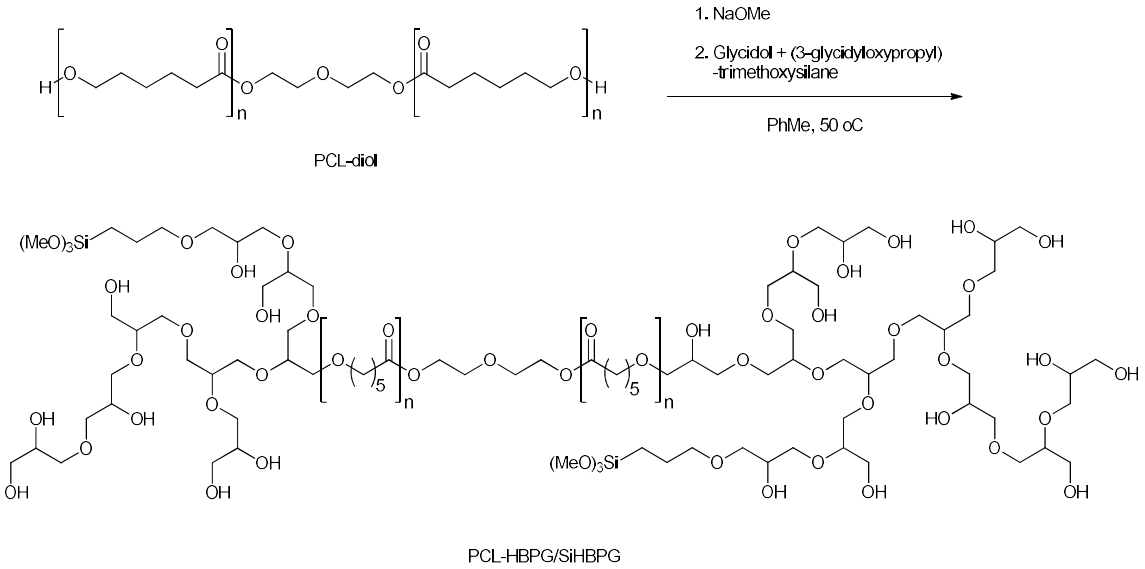

Scheme 1. Synthesis of the PCL-HBPG/SiHBPG copolymers.

Table 1. Characterisation data of the PCL-HBPG/SiHBPG copolymers.

Composition	Mw Theor. (g/mol)	[a]Mw (g/mol)		[a]PDI		HBPG content		SiHBPG content		[b]Mean DP of HBPG blocks	Si content		[d]T_g (°C)
		Low Mw fraction	High Mw fraction	Low Mw fraction	High Mw fraction	Theor. Mol %	[b]Exp. Mol %	Theor. Mol. %	[b]Exp. Mol %		Theor Wt.%	[c]Exp. Wt.%	
HBPG/ 1SiHBPG	4 000	3 700	-	1.82	-	-	-	1.0	0.8	54	0.4	0.5	-11
PCL-45HBPG/ 1SiHBPG	3 636	1 200	-	1.24	-	40	45	1.0	1.0	22	0.3	0.6	-24
PCL-56HBPG/ 1SiHBPG	4 545	[95]1 200	[5]13 000	1.25	1.13	50	56	1.0	1.0	34	0.3	0.6	-26
PCL-73HBPG/ 1SiHBPG	7 407	[92]1 700	[8]18 800	1.13	1.22	70	73	1.0	1.4	73	0.3	0.6	-22
PCL-90HBPG/ 1SiHBPG	20 000	[20]2 800	[80]25 000	1.15	1.30	90	90	1.0	0.6	242	0.4	0.5	-14

[a] Determined by GPC in H_2O/MeOH (90/10 v/v)

[b] Determined by ^1H NMR in DMSO-d_6

[c] Determined by TGA (see ESI)

[d]The glass transition temperatures were determined by DSC

[e] The area of the different fractions as percentages are presented as superscript on the particles' M_w

The copolymers' structural compositions were determined by FTIR and ^1H NMR in DMSO-d_6. The FTIR spectra of PCL, HBPG/1SiHBPG and PCL-73HBPG/1SiHBPG are shown in Fig. 1. The PCL spectra display characteristic peaks of C=O stretching vibrations at 1728 cm^{-1} (peak a), the $-CH_2$ and $-OCH_2$ bending modes between 2867 to 2946 cm^{-1} (peaks b) and the C−O−C stretching vibrations peaks at 1042, 1107 and 1233 cm^{-1} (peaks c). In the FTIR spectrum of HBPG/1SiHBPG the absorption band at 3442 cm^{-1} (peak d) is assigned to the terminal hydroxy groups in the polymer, whereas as in the PCL spectrum the methylene stretching bands appeared between 2946 and 2867 cm^{-1} (peaks b). The absorption bands at 1177 and 1240 cm^{-1} (peaks c) are attributed to the characteristic polyether C–O–C stretching vibrations of the repeating monomer units. The FTIR spectrum of PCL-73HBPG/1SiHBPG clearly shows peaks characteristic of both HBPG/1SiHBPG and PCL. Compared to the spectrum of the HBPG/1SiHBPG, for the PCL-73HBPG/1SiHBPG a new adsorption band attributed to the C=O stretching vibrations of the ester carbonyl group appears at 1728 cm^{-1}. The FTIR spectra of PCL-45HBPG/1SiHBPG, PCL-56HBPG/1SiHBPG and PCL-90HBPG/1SiHBPG are shown in Fig. 2S, ESI.

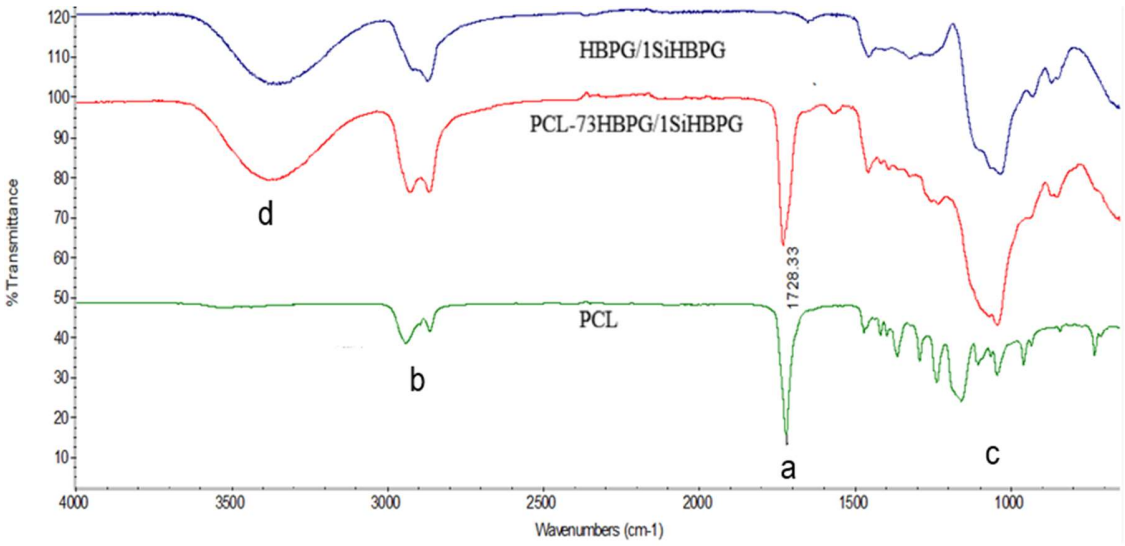

Fig. 1. FTIR spectra of PCL, PCL-73HBPG/1SiHBPG and HBPG/1SiHBPG.

The ^{1}H NMR spectrum of the PCL-56HBPG/1SiHBPG is shown in Fig. 2. The multiplets between δ = 3.40 – 3.80 ppm correspond to the CH and CH_2 protons of the HBPG and to OCH_3 groups of SiHBPG. The chemical shifts at δ = 4.25 ppm, δ = 2.30 – 2.50 and at δ = 1.20 – 1.70 are assigned to the methylene protons of $–(CH_2)_3–$, $–OCCH_2–$, and $–CH_2OOC–$ of the PCL moieties, respectively. The compositions of the PCL-HBPG/SiHBPG samples were calculated by examining the relative ratios of signal intensities of the methylene protons of PCL groups and the methyl and methylene protons of both HBPG and SiHBPG groups. The experimental values were in good agreement with the theoretical (Table 1). Given the convoluted method of measuring the experimental silicon content by using TGA (see ESI and Table 1), the agreement between the theoretical and experimental silicon content values is understandably not so good. However this could be considered reasonable.

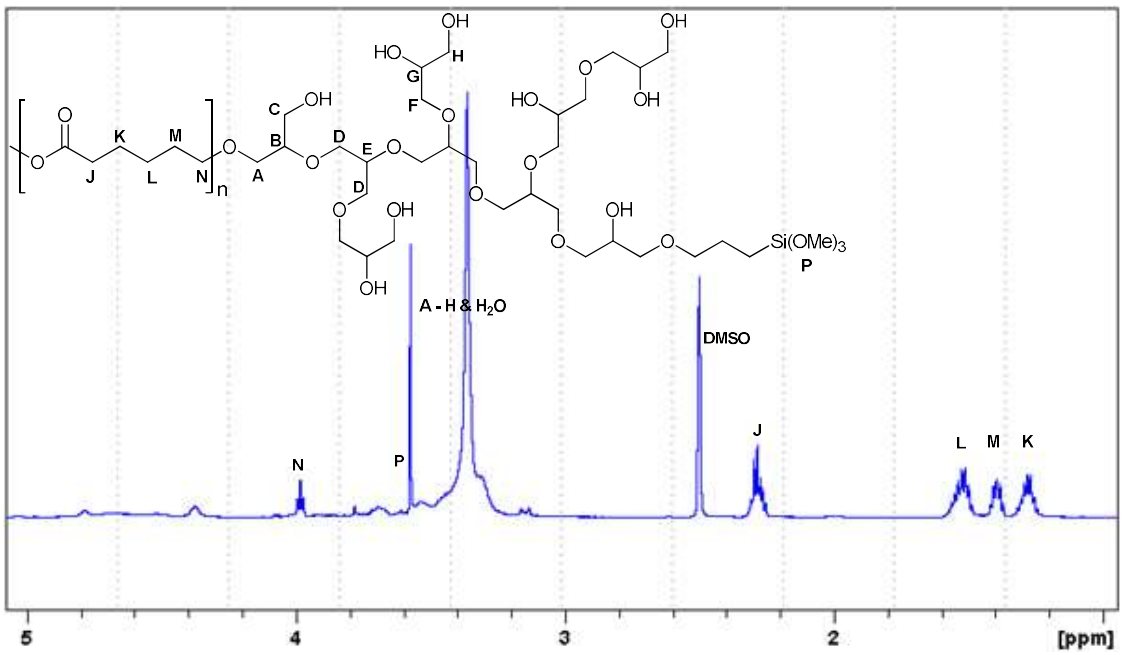

Fig. 2. ^{1}H NMR spectrum of PCL-56HBPG/1SiHBPG in DMSO-d_6.

Thermal properties and degradation. The melting and crystallization behaviour of the various PCL-HBPG/SiHBPG copolymers was investigated by DSC. The DSC thermograms of the starting PCL diol and representative PCL-HBPG/SiHBPG copolymers are shown in Fig. 3a and 3b, respectively. To eliminate the thermal history of the samples, all DSC curves shown in Fig. 3 represent the second cooling and heating. For PCL, each cycle includes a glass transition (T_g), endothermic during heating (melting), and exothermic during cooling (crystallization) transitions (Fig. 3a). The endotherm of the second melting for PCL is bimodal with peak maxima at T_{m1} = 39.0 °C and T_{m2} = 45.3 °C. The sample exhibited a single exothermic crystallization temperature at T_c = 20.5 °C. Previously, the presence of multiple melting peaks in the crystalline polystyrene samples were attributed to the melting of both less perfect (thinner or defect-containing) and a dominant thicker lamella during the heating cycle.[32] The thermograms for the PCL-HBPG/SiHBPG copolymers resemble that of HBPG/1SiHBPG where no melting or crystallization peaks were observed (Fig. 3b). This indicates that all PCL-HBPG/SiHBPG

copolymers were amorphous. The glass transition temperatures for all polymers are presented in Table 1. The data show that T_g increases as the HBPG content increases. For example, PCL-56HBPG/1SiHBPG T_g was –26 ºC, whereas for the PCL-90HBPG/1SiHBPG it was –14 ºC. The increase in T_g with increasing HBPG content was also observed for other similar systems.[33] It is well known that chain mobility has an important effect on T_g of a polymer. Any decrease in chain mobility as a result of cross-linking, inter- and intramolecular interactions, or changes in the copolymer composition, could result in an increase in T_g. For our systems, the increase in HBPG and SiHBPG content could result in a reduction in mobility and hence an increase in T_g owing to the increase in inter- and intra-chain hydrogen-bonding interactions between HBPG and SiHBPG moieties.[34]

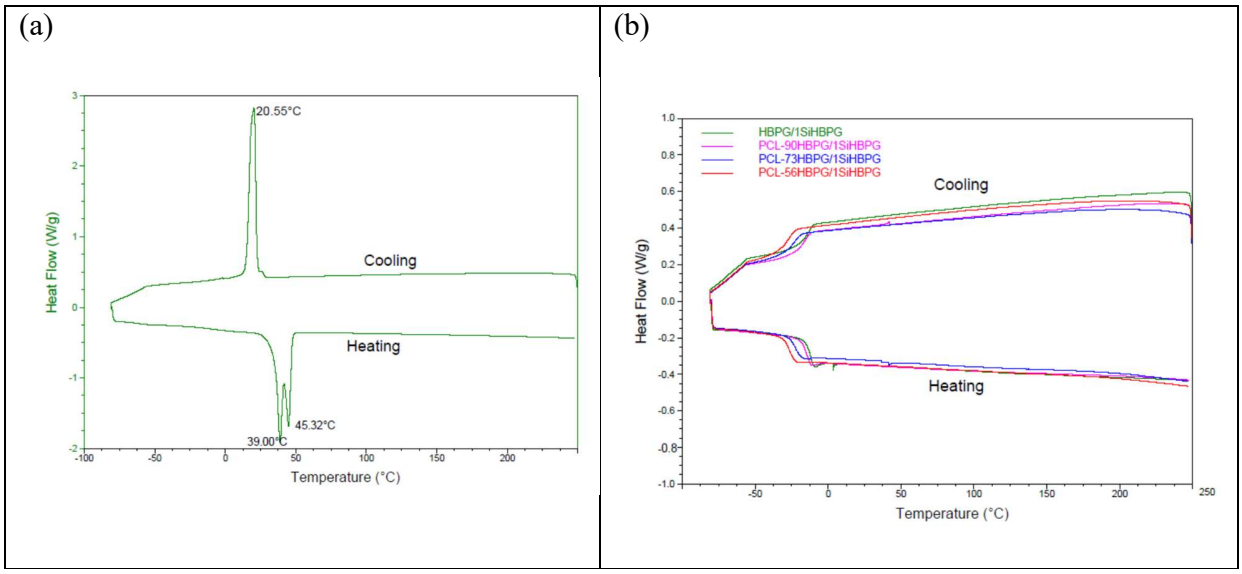

Fig. 3. DSC thermograms: (a) PCL diol 2000; (b) HBPG/1SiHBPG and PCL-HBPG/SiHBPG copolymers.

Aqueous solution properties. CAC determination, turbidimetry, SLS and SAXS measurements were conducted in order to study the phase transition and aggregation behaviour of the PCL-HBPG/SiHBPG in dilute aqueous solutions as a function of the HBPG content, concentration and temperature.

CAC determination. The PCL-HBPG/SiHBPG polymers are amphiphilic. They readily self-assemble in aqueous solution above certain critical concentrations. At low concentrations the PCL-HBPG/SiHBPG copolymers are freely dispersed in the solution. As the concentration increases, the free energy of the system also increases owing to unfavourable interactions between hydrophobic moieties and water molecules. Above a certain critical concentration, defined as CAC, the otherwise free amphiphilic species begin to aggregate into particles in order to minimise the free energy of the system, whereas at concentrations well above the CAC the particles start to agglomerate into larger particles and clusters. To determine the CAC of the PCL-HBPG/SiHBPG copolymers in aqueous solution, a previously described approach has been adopted utilising the nonpolar dye DPH, the absorption characteristics of which are sensitive to changes in its microenvironment. The dye shows minimal absorbance in water but a characteristic maximum at 356 nm is observed in a hydrophobic environment, such as upon solubilisation of DPH in the hydrophobic domains of the copolymer aggregates. The variation of the absorption of DPH at 356 nm with the concentration of PCL-56HBPG/1SiHBPG is presented in Fig. 4. The CAC values were determined from the break of the DPH absorbance *vs* copolymer concentration curves.

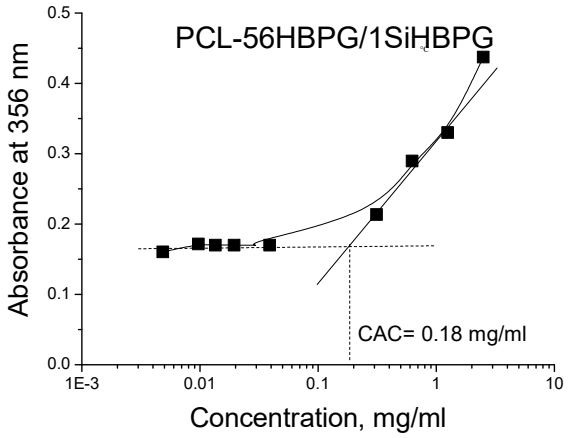

Fig. 4. Variations of the absorbance of DPH at 356 nm with concentration of PCL-56HBPG/1SiHBPG at 37 °C.

The CAC values were determined at four temperatures: 25, 37, 50 and 60 °C. The data is plotted as a function of temperature in Fig. 5a. The CACs of the copolymers were only slightly affected by temperature and were found to decrease with increasing temperature. The decrease of CAC with the increase in temperature is commonly observed in the aqueous solutions of polymers exhibiting lower critical solution temperatures, LCST, such as Pluronics and the analogous block copolymers based on linear PG and PPO (LGP-copolymers). [15, 16, 35] For the Pluronic copolymers the cmcs are known to decrease by an order of magnitude with a 10 °C increase in temperature. For the LGP copolymers the CAC was found to depend strongly upon the PG content and to be sensitive to temperature, although not as much as for the Pluronic copolymers. For the PCL-HBPG/SiHBPG, however, the decrese in CAC with increasing temperature is somehow unexpected as the PCL is hydrophobic over the entire temperature range, whereas as shown previously the solubility of the polyglycidol increases at elevated temperatures.[15, 16, 35] Therefore, we would expect an increase of CACs with increasing temperature. For non-ionic amphiphilic polymers in aqueous solution the CAC depends strongly upon the balance of two opposite thermally controlled molecular interactions. These are the hydrophobic effect of the nonpolar polymer units, which favours the micellization, and the steric repulsion between the hydrophilic segments. At lower temperatures, the PCL chains in PCL-HBPG/SiHBPG copolymers are covered by the HBPG/SiHBPG branches to decrease their unfavourable interactions with water. At elevated temperatures the solubility of polyglycidol increases and it expands into the aqueous phase to a greater extent, which weakens the steric protection of the HBPG/SiHBPG branches and results in exposure of the hydrophobic PCL chains to water. This

facilitates micelle aggregation and decreases the CAC. A similar phenomenon has been previously reported by Bakardzhiev et al.[36] for polyglycidol-derivatized lipids. In the present research, as the HBPG content increases the effects of temperature become less pronounced and for the most hydrophilic PCL-90HBPG/1SiHBPG the temperature dependence of the CAC is only modest. For example, for the PCL-45HBPG/1SiHBPG the CAC at 25 °C is three times higher than at 60 °C, whereas for the PCL-90HBPG/1SiHBPG the CAC at the lowest temperature is approximately 1.5 times higher (Fig. 5a).

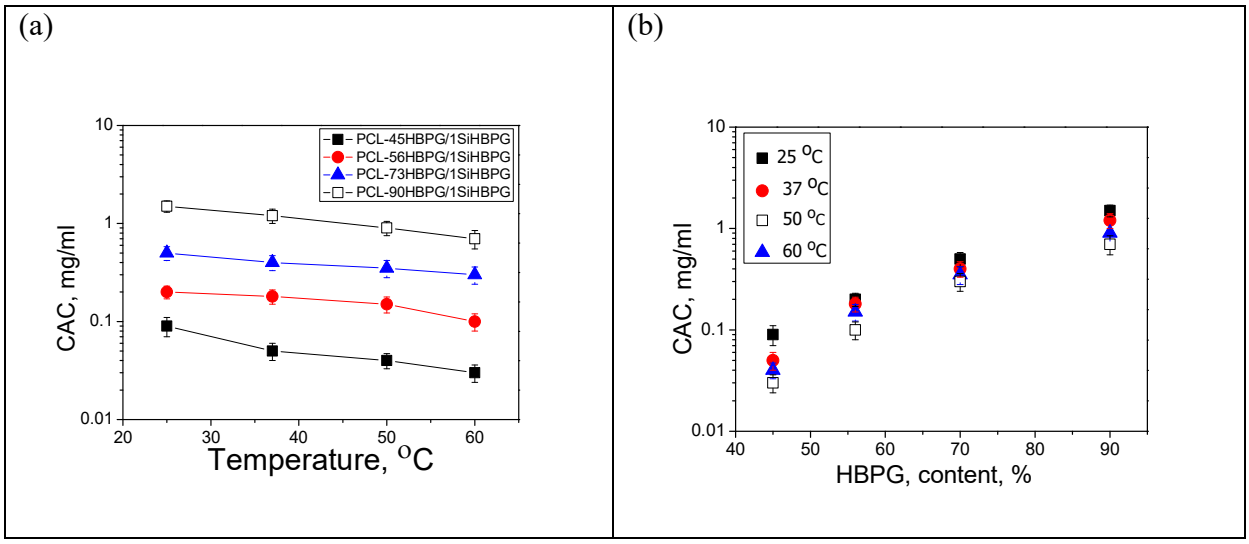

Fig. 5. The CAC as a function of (a) solution temperature and (b) HBPG content for PCL-HBPG/SiHBPG copolymers.

The CAC data for all polymers are re-plotted in Fig. 5b as a function of HBPG content. The CAC values show a gradual increase with increasing HBPG content, indicating that micelle formation becomes less favourable. For example, compared to PCL-73HBPG/1SiHBPG and PCL-90HBPG/1SiHBPG the CAC values at 25 °C for the most hydrophobic copolymer PCL-45HBPG/1SiHBPG are approximately five and ten times higher, respectively. Similarly to previous reports of the poly(ethylene glycol)-poly(ε-decalactone) copolymers, PEG-PεDL[37], the PCL-HBPG/SiHBPG copolymers will form micelles only when the hydrophobic effect

overcomes the bulky branched structure, resulting in higher CACs for the most hydrophilic copolymers. For the present PCL-HBPG/SiHBPG copolymers, the CAC values were in line with those reported previously for analogous systems based on star-like PCL-HBPG copolymers, PCL-s-HBPG.[27] Compared to the PCL23-s-HBPG6 and PCL51-s-HBPG6 (here the numbers next to the PCL and HBPG segments represent the degree of polymerization of the PCL and HBPG arms, respectively) that are characterised with shorter and longer PCL chain lengths, respectively, and similar numbers of repeating glycidol units per arm, the CAC values for our PCL-HBPG/SiHBPG copolymers are approximately two times lower. This could be attributed to the different structure of our copolymers. Indeed, at molecular weights ranging from 2,600 to 5,900 (DP = 23 – 51) the length of the PCL block appears to be of secondary importance in determining the CAC: PCL23-s-HBPG6 and PCL51-s-HBPG6 were found to have CAC values which differed by approximately 10%.[27] Another possible explanation for the lower values of CAC could be the effect of the SiHBPG moieties which make them more hydrophobic compared to the corresponding PCL-s-HBPG polymer.

Turbidity measurements To further explore the anomalous temperature behaviour in the aqueous solution of the PCL-HBPG/SiHBPG copolymers, the variation in light transmitted through dispersions of the copolymers with temperature was investigated. Representative transmittance versus temperature curves of the dilute aqueous dispersions at concentrations above the CAC of all copolymers are shown in Fig. 6. The variations in turbidity were strongly composition dependent. For the PCL-90HBPG/1SiHBPG the variations of transmittance with temperature resemble those observed with dilute aqueous solutions of HBPG/1SiHBPG. The solutions remained transparent and showed no temperature variations over the whole temperature range. The absence of temperature induced changes in the PCL-90HBPG/1SiHBPG solutions could be

related to improved steric shielding of the hydrophobic backbone with the largest HBPG branches. The dispersions of PCL-56HBPG/1SiHBPG and PCL-73HBPG/1SiHBPG were temperature sensitive and showed detectable critical temperatures at 11 and 19 °C, respectively, at which the transmittance started to decrease sharply upon heating. These curve patterns were reminiscent to a clouding process displayed by materials exhibiting LCST properties, however, full clouding in terms of formation of highly opalescent/opaque dispersions with transmittance of only a few percent, was not observed most probably due to the relatively high HBPG content. Slight gradual increases in transmittance were observed at elevated temperatures which were related to the increase in solubility of HBPG moieties. The dispersion of PCL-45HBPG/1SiHBPG, that is the copolymer with the lowest HBPG content, was opaque but homogeneous over the whole temperature range studied, suggesting the existence of large particles in the solutions. The slight gradual decrease in transmittance with increasing temperature can be attributed to prevailing effects of the hydrophobic moieties – PCL and trimethoxysilyl groups – which can contribute to shape transitions of hydrophobic domains and hydrophilic shell collapse both detected by SAXS (see below). The aqueous solution properties of PCL-45HBPG/1SiHBPG in some aspects resemble those observed previously in the corresponding LGP-copolymers with intermediate PG content, i.e LGP64 and LGP134. [15, 16, 35] The anomalous micellization behaviour of LGP64 and LGP134 has been explained in terms of the specific copolymer composition and/or delicate balance between PG and PPO blocks rather than the presence of hydrophobic contaminants. The aqueous solution properties of the PCL-45HBPG/1SiHBPG, however, are not so well defined probably due to the presence of trimethoxysilyl end-groups and/or the larger molecular weight distributions of the copolymers.

For the PCL-90HBPG/1SiHBPG the variations of transmittance with temperature resemble those observed with dilute aqueous solutions of HBPG/1SiHBPG. The solutions remained transparent and showed no temperature variations over the whole temperature range. The absence of temperature induced changes in the PCL-90HBPG/1SiHBPG solutions could be related to improved steric shielding of the hydrophobic backbone with the largest HBPG branches. The solutions of PCL-56HBPG/1SiHBPG and PCL-73HBPG/1SiHBPG were temperature sensitive and showed detectable critical temperatures between 11 and 19 °C at which the transmittance started to decrease sharply upon heating. These could be attributed to the critical temperatures at which the particle shells start to collapse (see SAXS results). Slight gradual increases in transmittance were observed at temperatures above 60 °C which were related to the increase in solubility of all copolymers. For the PCL-56HBPG/1SiHBPG the temperature interval for the transition from clear to opaque solutions was larger (approx. 24°C) compared to that of PCL-73HBPG/1SiHBPG (approx. 8 °C). This might be attributed to the more cooperative collapse of bigger copolymers with faster phase separation.

(a) (b)

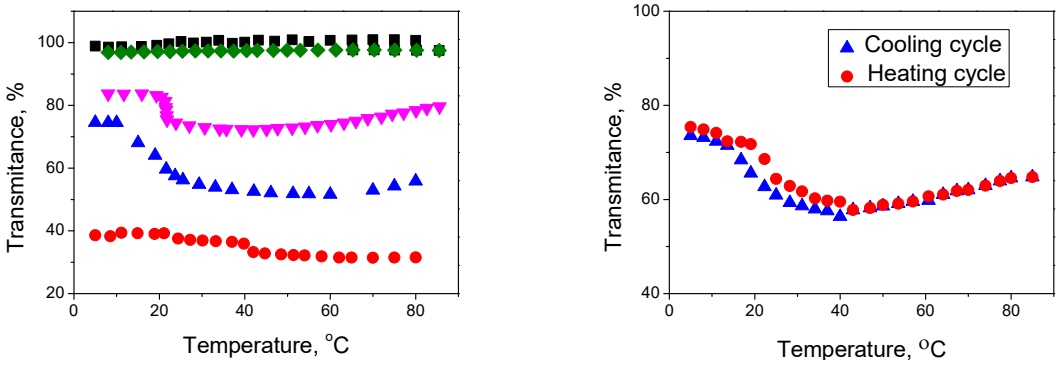

Fig. 6. (a) Turbidity measurements for the 5 mg/ml aqueous solutions of PCL-45HBPG/1SiHBPG (red circles); PCL-56HBPG/1SiHBPG (blue triangles); PCL-

73HBPG/1SiHBPG (magenta triangles); PCL-90HBPG/1SiHBPG (olive diamonds) and HBPG/1SiHBPG (black squares); (b) transmittance versus temperature curves in heating/cooling cycles for the 5mg/ml aqueous solutions of PCL-56HBPG/1SiHBPG.

For the aqueous solutions of PCL-56HBPG/1SiHBPG the variations of the transmittance with the temperature during a heating/cooling cycle over an interval of 5 – 80 °C are shown in Fig. 6b. The observed phase transitions of the copolymer were fully reversible, exhibiting only a very small hysteresis. Whereas the heating/cooling curves completely overlap at high temperatures a slight difference in the transmittance (<6% transmittance) during the cooling cycle was observed at temperatures between 19 and 37 °C. The occurrence of hysteresis in heating/cooling cycles for some PEG-based amphiphilic copolymers has been previously attributed to hydrophobic effect driven aggregation requiring conformational rearrangement before re-dissolution of the aggregates.[38] Another possible explanation for the hysteresis could be the formation of hydrogen bonds as observed previously for some PNIPAM-based polymer systems.[39] Previously, Miasnikova et al.[40] reported that the architecture of amphiphilic block copolymers has an effect on the kinetics of re-swelling/re-dissolution of the aggregates when passing through the phase transition in heating/cooling cycles. Star and triblock copolymers tended to have a decreased rate of re-swelling, giving rise to a hysteresis effect.

SLS measurements. SLS experiments were conducted at concentrations above the CACs in order to determine the weight average molar masses (M_w) and the corresponding aggregation numbers (N_{agg}), radii of gyration (R_g), and second virial coefficients (A_2) of the particles formed in aqueous solution of representatives of the copolymers with low and high HBPG contents – PCL-56HBPG/1SiHBPG and PCL-90HBPG/1SiHBPG, respectively. The Zimm plot method was used for the evaluation of the SLS parameters of the systems. A typical Zimm plot of PCL-

90HBPG/1SiHBPG is presented in Fig. 7. The SLS parameters for PCL-56HBPG/1SiHBPG and PCL-90HBPG/1SiHBPG at temperatures of 25 and 60 °C are collected in Table 2. As seen from Table 2, the molar masses ranged from 0.148×10^6 – 4.669×10^6 $gmol^{-1}$, corresponding to aggregation numbers from 7 to about 1000 macromolecules per particle. N_{agg} and R_g of the particles formed from the more hydrophilic copolymer (PCL-90HBPG/1SiHBPG) were only slightly affected by temperature, whereas the value of A_2 was almost doubled indicating improvement of the particle-solvent interactions upon increasing temperature.

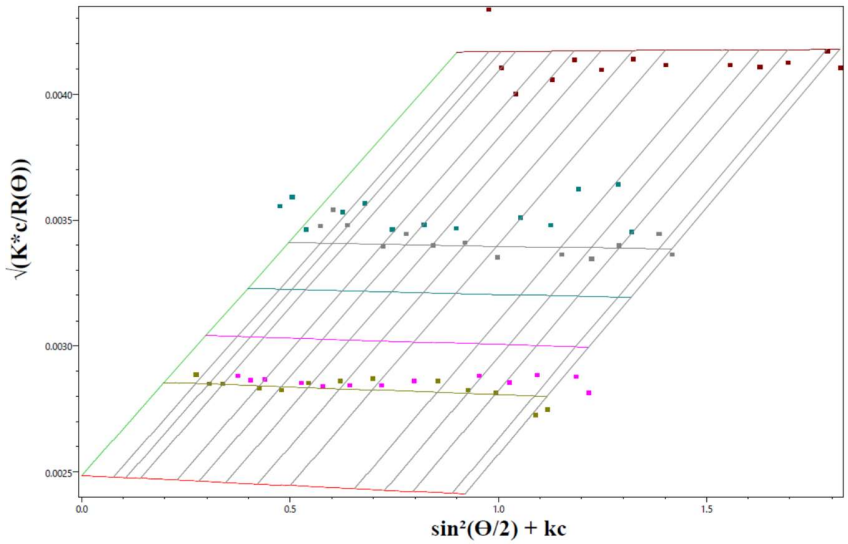

Fig. 7. Zimm plot of PCL-90HBPG/1SiHBPG in water at 60 °C.

The effect of temperature on the molar mass and, hence, aggregation number of the particles of PCL-56HBPG/1SiHBPG was more pronounced. The reduction of these parameters by more than 50% could be associated with enhanced exposure of larger parts of the PCL moieties to the aqueous environment (contributing to the larger decrease in CACs for the copolymers of lower HBPG content, see above Fig. 5a and related discussion), which was expected to reflect in formation of more compact and tight particles because of the increased hydrophobicity of the

PCL moieties. The rise in temperature influenced HBPG moieties in a somewhat unexpected manner: they became more hydrophilic[15, 16, 35] and thereby larger in size because of the more favourable interactions with water thus increasing their repulsive action, which ultimately lead to a decrease in total molar mass and N_{agg}. However, decrease in molar mass and N_{agg} hardly corresponded to the drop in transmittance of the dispersion (Fig. 6) but could be rationalized in terms of changes in the internal structure of the particles and shape transition of the PCL domains (vide infra). Table 2 also indicated a very slight decrease in R_g and doubling of the A_2 value as observed for the more hydrophilic copolymer. Single-angle/single-concentration measurements of the hydrodynamic radii from dynamic light scattering gave results consistent with those for R_g. Representative particle size distributions showing a lack of large aggregate fractions are displayed in Fig. 4S – 6S, ESI.

Table 2. Static light scattering parameters of selected copolymers in water at different temperatures and concentrations of PCL-56HBPG/1SiHBPG ranging from 2.7 × 10^{-2} – 2.5 mg/ml and of 1.7 – 33 mg/ml for PCL-90HBPG/1SiHBPG.

Copolymer	***T*** **(°C)**	$10^6 \times Mw$ ***(g mol^{-1})***	$10^{-5} \times A_2$ **(mol mL g^{-2})**	R_g **(nm)**	N_{agg}
PCL-90HBPG/1SiHBPG	25 °C	0.148 ± 0.059	5.996 ± 0.160	23 ± 0.5	7
PCL-90HBPG/1SiHBPG	60 °C	0.184 ± 0.057	10.16 ± 0.150	24 ± 0.5	9
PCL-56HBPG/1SiHBPG	25 °C	4.669 ± 0.103	2.352 ± 0.266	55 ± 0.2	1 027
PCL-56HBPG/1SiHBPG	60 °C	2.289 ± 0.110	5.471 ± 0.263	49 ± 0.2	503

SAXS analysis. The obvious question that arises from these results concerns the internal structure of the particles formed by the PCL-HBPG/SiHBPG copolymers, particularly those of the lower HBPG content. They cannot be the familiar core-corona micelles, because of their large

dimensions (larger than the length of a fully stretched macromolecule) and aggregation numbers (typical for non-micellar aggregates). To answer this question, the aqueous dispersions of the copolymers were studied by SAXS.

SAXS experiments were performed at 30 and 60 °C for PCL-HBPG/SiHBPG copolymers at concentrations of 0.5 mg/ml. Representative SAXS profiles for PCL-45HBPG/1SiHBPG, PCL-56HBPG/1SiHBPG, PCL-73HBPG/1SiHBPG and PCL-90HBPG/1SiHBPG at lower and higher temperatures are shown in Fig. 8 and Fig. 7S, ESI. The scattering data were first analysed by slope determination (i.e. $I(q) \sim q^{-\alpha}$); the slopes at low (0.01 – 0.03 $Å^{-1}$) and large (0.01 – 0.25 $Å^{-1}$) q ranges were calculated and are summarized in Table 3. For the PCL-45HBPG/1SiHBPG and PCL-56HBPG/1SiHBPG copolymers at low q ranges, strong scattering was observed. This could be attributed to the traces of scattering from the large particles ($>1/m_{an}$), which is in good agreement with the SLS results. The data at intermediate and large q ranges indicates scattering from small objects (<16 nm approx.), for which it is reasonable to assume that these are the PCL domains. On the q scale of the SAXS measurements no scattering from non-associated Gaussian chains was observed, which may imply that all copolymer chains self-associate and the PCL domains are the main scattering objects. For the PCL-73HBPG/1SiHBPG and PCL-90HBPG/1SiHBPG copolymers, scattering from relatively small objects was detected and this is in good agreement with the SLS results (Table 2).

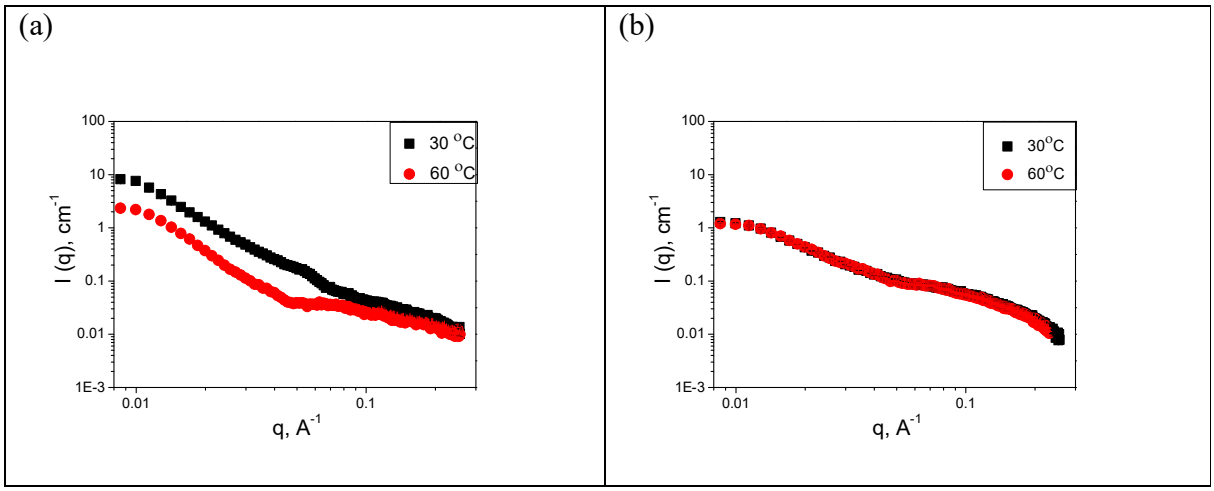

Fig. 8. SAXS profiles obtained from 0.5 mg/ml aqueous dispersions of (a) PCL-45HBPG/1SiHBPG and (b) PCL-90HBPG/1SiHBPG at 30 °C and 60 °C.

Table 3. Values of the slopes determined as $I(q) \sim q^{-\alpha}$ at different q ranges, scattering at zero angle (I(0)), radius of gyration (R_g), finite maximal dimensions of the domains (D_{max}) for 0.5 mg/ml aqueous dispersions.

Copolymer	**T (°C)**	**Slopes at *q* ranges:**		**R_g (Å)**	**I(0) (cm^{-1})**	**D_{max} (Å)**
		0.01-0.03	**0.01-0.25**			
PCL-45HBPG/1SiHBPG	30	2.62 ± 0.02	1.40 ± 0.02	164 ± 1.3	17.0 ± 0.2	500
PCL-45HBPG/1SiHBPG	60	2.75 ± 0.02	1.37 ± 0.02	150 ± 2	4.4 ± 0.2	450
PCL-56HBPG/1SiHBPG	30	2.39 ± 0.02	3.00 ± 0.02	158 ± 1.5	12.7 ± 0.1	500

PCL-56HBPG/1SiHBPG	60	2.59 ± 0.02	2.78 ± 0.02	162 ± 1	16.3 ± 0.1	500
PCL-73HBPG/1SiHBPG	30	1.77 ± 0.02	1.83 ± 0.02	115 ± 1.6	2.6 ± 0.1	350
PCL-90HBPG/1SiHBPG	30	1.80 ± 0.02	1.70 ± 0.02	120 ± 4	1.9 ± 0.1	400
PCL-90HBPG/1SiHBPG	60	1.80 ± 0.02	1.70 ± 0.02	111 ± 2	1.8 ± 0.1	350

The scattering curves were converted into real space equivalents, pair distance distribution function, p(r), by the Indirect Fourier Transformation (IFT) procedure developed by Glatter et al.[41] Previously, IFT has been successfully applied to describe the aqueous solution properties of a range of polymer and surfactant systems.[42] Details of this analysis are presented in the ESI. The IFT requires only limited information on the maximum dimensions of the objects (D_{max}) and on the possible shapes of the aggregates: sphere-like (all three dimensions are of same length scale), rod-like (one size dimension is much larger than the other two), or sheet-like (one dimension is small relative to the other two).[41, 43] Fig. 9 shows the evolution of the normalized p(r) functions (for better comparison data have been normalized by maximum valued of p(r) i.e., p_{max} and r has been normalied by d_{max} used in IFT treatment) with temperature for 0.5 mg/ml dispersions of all copolymers at 30 and 60 °C. Application of IFT enabled us to calculate the shape of the p(r), from which it is possible to calculate I(0) (scattering at "zero angle") and R_g (radius of gyration of scattering contrast within the aggregate). The values of these two quantities for each copolymer are shown in Table 3. R_g is related to the size of the PCL domains

and HBPG/1SiHBPG corona and the distribution of scattering length density within these structures. An interesting finding is that for the PCL-45HBPG/1SiHBPG, which is the most hydrophobic copolymer, the dimensions of the domains decrease slightly with increasing temperature, which is in agreement with the suggestion of formation of more compact and tight particles/domains at elevated temperatures (see the previous section).

For the rest of the copolymers there was no significant alteration in the size of the scattering objects at any temperature tested. At low and high temperatures (Fig. 9b–d) the scattering profiles from the solutions of these copolymers are similar and fall into a common master curve. This is also consistent with the SLS data which for the PCL-90HBPG/1SiHBPG copolymer showed doubling of the A_2 values at higher temperatures without changes in the other light scattering parameters (see Table 2). Furthermore, this finding is in good agreement with the turbidity measurements where optically clear solutions were observed for the most hydrophilic PCL-73HBPG/1SiHBPG and PCL-90HBPG/1SiHBPG polymers. The p(r) functions of the most hydrophilic copolymers, PCL-73HBPG/1SiHBPG and PCL-90HBPG/1SiHBPG, clearly show scattering from core-shell structures. They are characterized by two maxima at short and long distances at both low and high temperatures. The first maximum is attributed to the scattering from compact PCL domains, whereas the second can be attributed to scattering from the corona (consisting of HBPG/SiHBPG branches) which becomes more compact as the temperature increases. For lower contents of HBPG, the p(r) functions show only one maximum. A possible reason for this is that the HBPG shell is not so well separated from its PCL core and/or the scattering contribution is not so high. As with any numerical solution which requires an additional stabilization parameter, the IFT results should be checked with direct modelling.

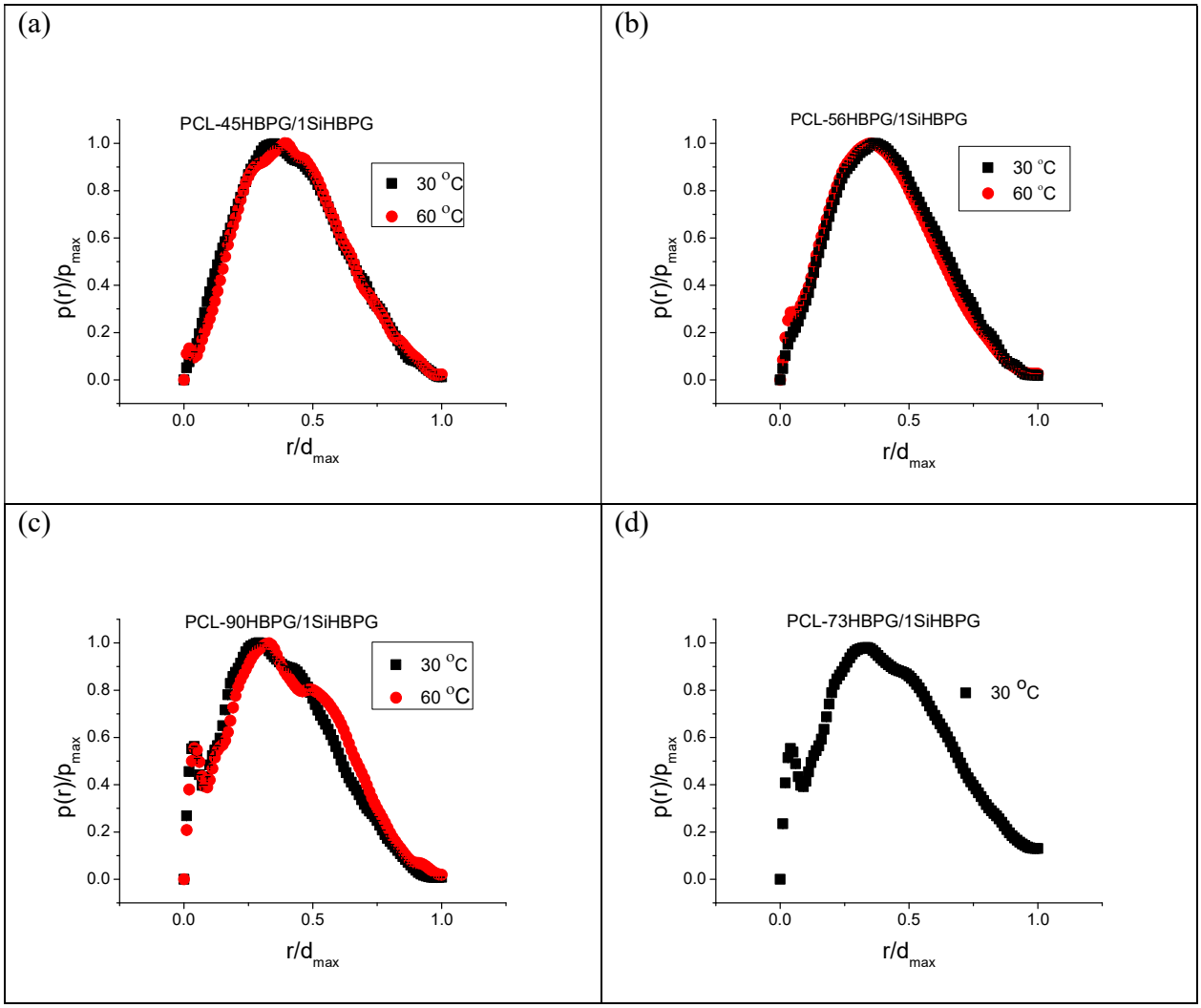

Fig. 9. Normalized pair distances distribution functions, $p(r/d_{max})/p_{max}$ vs r/d_{max}, for 0.5 mg/ml solutions of (a) PCL-45HBPG/1SiHBPG; (b) PCL-56HBPG/1SiHBPG; (c) PCL-90HBPG/1SiHBPG at 30 and 60 °C and (d) PCL-73HBPG/1SiHBPG at 30 °C.

The high q ranges ($q > 0.06$ Å^{-1}) of the scattering curves were fitted to a simple model of an ellipsoid of revolution with axes a, b, b. The results for the parameters of the core for the aqueous solutions of PCL-HBPG/SiHBPG copolymers at different temperatures are presented in Table 4. The analysis has been performed under the assumption that the sizes of the cores and the shells of the aggregates formed in the aqueous solutions are very different and at high q interval

there is a contribution only from the cores. The obtained parameters, however, could be affected by the trace scattering from the shell.

Table 4. Analysis of large q part (q>0.06 Å^{-1}) with elliposoid of revolution model.

Copolymer	**T °C**	**a Å**	**b Å**	**V Å^3**	**N_{aggPCL}**	**$N_{domains}$**
PCL-45HBPG/1SiHBPG	30	Fixed 100	5.8±0.1	14091	5	-
PCL-45HBPG/1SiHBPG	60	43±5	5.4±0.3	5252	2	-
PCL-56HBPG/1SiHBPG	30	50±2	13.2±0.1	36492	12	86
PCL-56HBPG/1SiHBPG	60	59±9	14.9±0.5	54800	18	28
PCL-73HBPG/1SiHBPG	30	45±2	9.3±0.5	16303	5	-
PCL-90HBPG/1SiHBPG	30	31±1	5.6±1.7	4072	1	7
PCL-90HBPG/1SiHBPG	60	34±1	5.9±2.0	4957	2	5

Values of major semi-axis of the core, a, minor semi-axis of the core b, volume (V), and aggregation number (N_{aggPCL}) of the PCL domains, number of PCL domains ($N_{domains}$) in the large particles formed in water for the 0.5 mg/ml aqueous solution of PCL-HBPG/SiHBPG copolymers at different temperatures.

The scattering data were fitted to a model of core-shell ellipsoid with rotation axis a, b, b. The results for the parameters of the core and shell, i.e. major semi-axis of the core, a_c, minor semi-

axis of the core b_c, scattering length density of the core ρ_c; major semi-axis of the shell, A_{sh}, minor semi-axis of the shell, B_{sh}, the scattering length density of the shell ρ_{sh} and polydispersity of the shell thickness, PD_{sh} for the aqueous solutions of PCL-HBPG/SiHBPG copolymers at different temperatures and concentrations are presented in Table S1 of Supporting Info as possible scenario due to corlation between scattering contrast and structural parameters of core and shell structures.

The changes in the internal structure of the particles are schematically presented in Scheme 2. Similar behaviour has been previously observed for some Pluronic copolymers and other analogous polymers containing PG for which sphere-to-rod transition is typically observed upon increasing temperature[44] and could be associated with the drop of the transmittance (see Fig. 7 and related discussion). For the particles of the most hydrophilic copolymer, PCL-90HBPG/1SiHBPG, heating to 60 °C was not associated with dramatic changes in the internal structure and shape transitions of the PCL domains in particular.

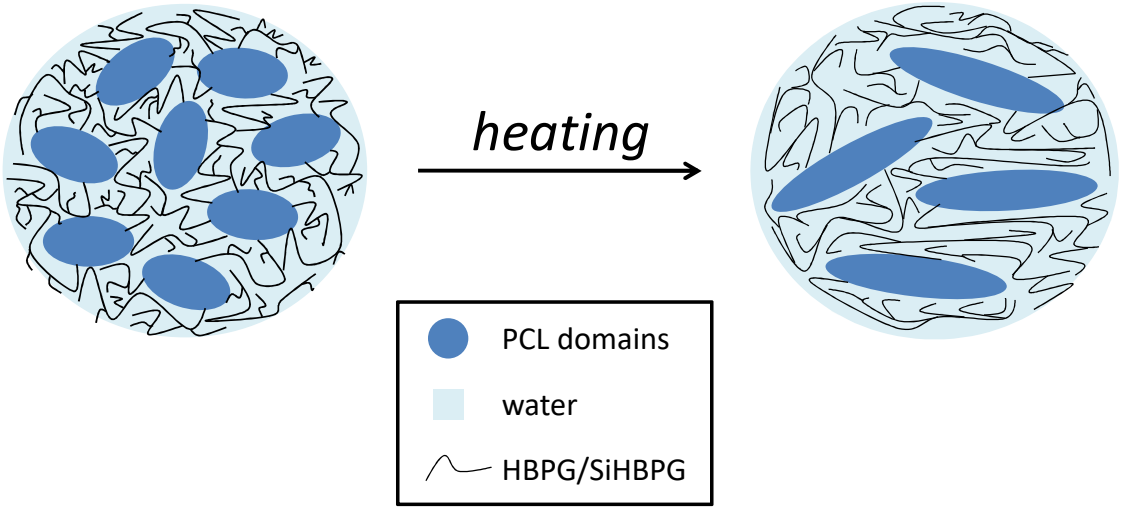

Scheme 2. Schematic presentation of the changes in the internal structure of the particles formed by PCL-56HBPG/1SiHBPG upon heating.

The values of a and b were used to calculate the domain volumes, V (Table 4). Assuming that the domains are entirely built by PCL and all PCL is in the domains, although some penetration of the SiHBPG moieties could be anticipated on the base of the hydrophobicity of the materials the aggregation number (N_{agg}) of the PCL domains (the number of PCL chains in one domain) can be estimated from the volume of the domain and the volume of a PCL chain. The latter was calculated based on the molecular weight and density of the PCL diol, which has been used as a starting material for the synthesis of the copolymers. The volume of PCL which contains approximately 18 caprolactone units was estimated to be 3100 $Å^3$. The number of PCL domains per large particle ($N_{domains}$) could be estimated by combining the light scattering and SAXS data. $N_{domains}$ was estimated by dividing the aggregation number of the large particles determined by SLS, N_{agg} (Table 2) by the aggregation number of the PCL domains, N_{aggPCL}. The resulting values are presented in Table 4. In general, the N_{aggPCL} of the domain decreases as the HBPG/SiHBPG content increases which is in agreement with the SLS results (Table 2). For the PCL-45HBPG/1SiHBPG and PCL-56HBPG/1SiHBPG the dramatic change of $N_{domains}$ upon heating reflects the changes of the solvent quality. At high temperatures the solubility of the HBPG increases and results in exposure of the whole hydrophobic PCL chain to water. This facilitates micelle aggregation, and decreases the CAC (see Fig. 6) which in turn increases the volume of the domain and the N_{aggPCL}. For PCL the solvent quality is not affected by changes in the temperature, however for HBPG/SiHBPG it gradually improves and leads to a decrease in $N_{domains}$ (Table 4). As the HBPG content increases the effect of temperature became less pronounced and for the PCL-73HBPG/1SiHBPG and PCL-90HBPG/1SiHBPG the N_{aggPCL} and $N_{domains}$ remain largely unaffected by the changes in the temperatures. The SAXS data confirmed the multicore structure of the particles, which facilitates a homogeneous distribution of material

(particularly PCL) in the scaffold. This is a very important advantage of the present copolymers, which is related to their potential as injectable scaffolds. Furthermore, the formation of stable multicore structures with collapsible shells as a result of the hydrophobic interactions between trimethoxysilyl end-groups (as detected by SAXS and turbidimetry) could promote the Si–O–Si crosslinking process and formation of covalently-linked gels.

Concluding remarks:

Herein we describe the synthesis and characterisation of a range of new PCL-HBPG/SiHBPG copolymers which will be further utilised for development of injectable gel scaffolds for tissue repair. The PCL-HBPG/SiHBPG were synthesised by anionic polymerization of a mixture of glycidol and (3-glycidyloxypropyl)trimethoxysilane using partially deprotonated PCL diol (molecular weight = 2000 g/mol) as a macroinitiator. A number of polymerizations were carried out to prepare PCL-HBPG/SiHBPG copolymers with a constant molar mass of the PCL middle block and HBPG/SiHBPG contents varying from 45 – 90 mol% for the HBPG and from 0.6 – 1.4 mol% for the SiHBPG, respectively. The thermal and degradation properties of PCL-HBPG/SiHBPG were investigated by TGA and DSC and the results compared with those of the corresponding HBPG/1SiHBPG and PCL polymers. For the PCL-HBPG/SiHBPG copolymers the increase in HBPG and SiHBPG content resulted in an increase in T_g owing to the increase in inter- and intra-chain hydrogen-bonding interactions between HBPG and SiHBPG moieties. The effects of the temperature and copolymer composition on the aqueous solution-phase behaviours of these copolymers were investigated over a range of temperatures. The PCL-HBPG/SiHBPG copolymers self-assembled above a CAC and formed multicore particles composed of compact PCL domains and HBPG/SiHBPG corona. The CAC values were found to decrease with

increasing temperature and decreasing the content of the hydrophilic component. The particles formed from the more hydrophilic copolymers (PCL-73HBPG/1SiHBPG and PCL-90HBPG/1SiHBPG) were only slightly affected by temperature and no significant alteration in their R_g and N_{agg} was observed at any temperature tested. The PCL-45HBPG/1SiHBPG and PCL-56HBPG/1SiHBPG, the most hydrophobic copolymers, formed more compact and tight particles/domains at elevated temperatures because of the enhanced exposure of larger parts of the PCL moieties to the aqueous environment. Furthermore a phase transition from ellipsoidal shape of the PCL domains to more elongated morphology was observed for PCL-56HBPG/1SiHBPG, upon heating to 60 °C. By combining SLS data and the SAXS results the $N_{domains}$ per large particle was estimated. For the more hydrophobic polymers the dramatic decrease in $N_{domains}$ upon heating reflected the changes of the solvent quality. The improved solubility of the HBPG at higher temperatures results in exposure of the whole hydrophobic PCL chain to water. This facilitates micelle aggregation and results in an increase in the volume of the domain and the N_{aggPCL}. The numerous hydrogen-bonds from the HBPG moieties as well as the Si–O–Si bonds were found to stabilise the particles. The gradual hydrolysis (and subsequent Si–O–Si crosslink formation) of trimethoxysilyl groups in PCL-HBPG/SiHBPG at higher concentrations could facilitate the formation of covalently-linked gels that would exhibit gradually increasing mechanical strength over time. The presence of the numerous hydroxyl groups in PCL-HBPG/SiHBPG could promote a positive biological response. The research offers the possibility to control the gels' mechanical properties, porosities, the cellular attachment and differentiation by tuning their copolymer compositions, architectures and extents of crosslinking. The gels' properties and performance will be described in separate forthcoming publications.

Supplementary Information (ESI) available. Polymer characterisation data and SAXS analysis data.

Author Information

Corresponding Author: *e-mail: S.Halacheva@bolton.ac.uk; S_Halacheva@yahoo.com

Acknowledgment: We are grateful to the EPSRC for financial support (EP/M02881X/1). The SAXS study was supported by the European Commission under the sixth Framework Programme through the Key Action: Strengthening the European Research Area, Research Infrastructures (Contract RII3-CT-2003-505925, Grant Agreement No. 226507-NMI3).

Data availability. The raw/processed data required to reproduce these findings cannot be shared at this time as the data also forms part of an ongoing study.

References:

[1] F. J. O'Brien, Biomaterials & scaffolds for tissue engineering, Mater. Today, 14 (2011) 88-95. https://doi.org/10.1016/S1369-7021(11)70058-X

[2] M. Sokolsky-Papkov, K. Agashi, A. Olaye, K. Shakesheff, A. J. Domb, Polymer carriers for drug delivery in tissue engineering, Adv. Drug Deliv. Rev, 59 (2007) 187-206. https://doi.org/10.1016/j.addr.2007.04.001

[3] R. Lanza, R. Langer and J. Vacanti, Eds. Principles of Tissue Engineering (Fourth Edition), Academic Press, Boston, 2014, pp. iii. https://www.elsevier.com/books/principles-of-tissue-engineering/lanza/978-0-12-370615-7

[4] E. Malikmammadov, T.E. Tanir, A. Kiziltay, V. Hasirci, N. Hasirci, PCL and PCL-based materials in biomedical applications, J. Biomater. Sci. Polym. Ed., 29 (2018) 863-893. https://doi.org/10.1080/09205063.2017.1394711

[5] Z. Li, B.H. Tan, Towards the development of polycaprolactone based amphiphilic block copolymers: molecular design, self-assembly and biomedical applications, Mater. Sci. Eng. C.: C, 45 (2014) 620-634. https://doi.org/10.1016/j.msec.2014.06.003

[6] S. Fu, P. Ni, B. Wang, B. Chu, L. Zheng, F. Luo, J. Luo, Z. Qian, Injectable and thermo-sensitive PEG-PCL-PEG copolymer/collagen/n-HA hydrogel composite for guided bone regeneration, Biomaterials, 33 (2012) 4801-4809. https://doi.org/10.1016/j.biomaterials.2012.03.040

[7] T. Cai, M. Li, B. Zhang, K.-G. Neoh, E.-T. Kang, Hyperbranched polycaprolactone-click-poly(N-vinylcaprolactam) amphiphilic copolymers and their applications as temperature-responsive membranes, J. Mat. Chem. B, 2 (2014) 814-825. https://doi. org/10.1039/C3TB20752H

[8] D. Mondal, M. Griffith, S.S. Venkatraman, Polycaprolactone-based biomaterials for tissue engineering and drug delivery: Current scenario and challenges, , Int. J. Polym. Mater. Polym Biomaterials, 65 (2016) 255-265. https://doi.org/10.1080/00914037.2015.1103241

[9] R.K. Kainthan, J. Janzen, E. Levin, D.V. Devine, D.E. Brooks, Biocompatibility Testing of Branched and Linear Polyglycidol, Biomacromolecules, 7 (2006) 703-709. https:// pubs.acs.org /**doi**/10.1021/bm0504882

[10] M. Calderón, M. A. Quadir, S.K. Sharma, R. Haag, Dendritic Polyglycerols for Biomedical Applications, Adv. Mater, 22 (2010) 190-218. https://doi.org/10.1002/adma.200902144

[11] A. Thomas, S. S. Müller, H. Frey, Beyond Poly(ethylene glycol): Linear Polyglycerol as a Multifunctional Polyether for Biomedical and Pharmaceutical Applications, Biomacromolecules, 15 (2014) 1935-1954. https://pubs.acs.org /doi/10.1021/bm5002608

[12] J.M. Curran, R. Chen, J.A. Hunt, Controlling the phenotype and function of mesenchymal stem cells in vitro by adhesion to silane-modified clean glass surfaces, Biomaterials, 26 (2005) 7057-7067. https://doi.org/10.1016/j.biomaterials.2005.05.008

[13] D. Wilms, F. Wurm, J. Nieberle, P. Böhm, U. Kemmer-Jonas, H. Frey, Hyperbranched Polyglycerols with Elevated Molecular Weights: A Facile Two-Step Synthesis Protocol Based on Polyglycerol Macroinitiators, Macromolecules, 42 (2009) 3230-3236. https://pubs.acs.org/doi/10.1021/ma802701g

[14] F. Wurm, J. Nieberle, H. Frey, Synthesis and Characterization of Poly(glyceryl glycerol) Block Copolymers, Macromolecules, 41 (2008) 1909-1911. https://pubs.acs.org/doi/10.1021/ma702458g

[15] S. Halacheva, S. Rangelov, C. Tsvetanov, Poly(glycidol)-Based Analogues to Pluronic Block Copolymers. Synthesis and Aqueous Solution Properties, Macromolecules, 39 (2006) 6845-6852. https://pubs.acs.org/doi/abs/10.1021/ma061040b

[16] S. Halacheva, S. Rangelov, C. Tsvetanov, Synthesis of Polyglycidol-Based Analogues to Pluronic L121−F127 Copolymers. Self-Assembly, Thermodynamics, Turbidimetric, and Rheological Studies, Macromolecules, 41 (2008) 7699-7705. https://pubs.acs.org/doi/abs/10.1021/ma801086b

[17] K. Helmut, M. Martin, Synthesis and degradation of biomedical materials based on linear and star shaped polyglycidols, J. Polym. Sci. A: Polym. Chem., 47 (2009) 3209-3231.

[18] M. Schömer, C. Schüll, H. Frey, Hyperbranched aliphatic polyether polyols, J. Polym. Sci. A: Polym. Chem., 51 (2013) 995-1019. https://doi.org/10.1002/pola.23359

[19] A. Sunder, R. Hanselmann, H. Frey, R. Mülhaupt, Controlled Synthesis of Hyperbranched Polyglycerols by Ring-Opening Multibranching Polymerization, Macromolecules, (1999), 32,

4240–4246. https://pubs.acs.org/doi/10.1021/ma990090w

[20] J. Xu, J. Yang, X. Ye, C. Ma, G. Zhang, S. Pispas, Synthesis and properties of amphiphilic and biodegradable poly(ε-caprolactone-co-glycidol) copolymers, J. Polym. Sci. A: Polym. Chem., 53 (2015) 846-853. https://doi.org/10.1002/pola.27515

[21] T. Cai, M. Li, K.-G. Neoh, E.-T. Kang, Surface-functionalizable membranes of polycaprolactone-click-hyperbranched polyglycerol copolymers from combined atom transfer radical polymerization, ring-opening polymerization and click chemistry, J. Mat. Chem. B, 1 (2013) 1304-1315. doi:10.1039/C2TB00273F

[22] Y. J. Kim, B. Kim, D. C. Hyun, J. W. Kim, H. E. Shim, S. W. Kang, U. Jeong, Photocrosslinkable Poly(ε-caprolactone)-b-Hyperbranched Polyglycerol (PCL-b-hbPG) with Improved Biocompatibility and Stability for Drug Delivery, Macromol. Chem. Phys., 216 (2015) 1161-1170. https://doi.org/10.1002/macp.201500047

[23] S. Sterman, J. G. Marsden, Silane coupling agents, Ind. Eng. Chem, 58 (1966) 33-37. https://pubs.acs.org/doi/abs/10.1021/ie50675a010

[24] A. Sosnik, D. Cohn, Ethoxysilane-capped PEO–PPO–PEO triblocks: a new family of reverse thermo-responsive polymers, Biomaterials, 25 (2004) 2851-2858. https://doi.org/10.1016/j.biomaterials.2003.09.057

[25] A. Dworak, G. Baran, B. Trzebicka, W. Wałach, Polyglycidol-block-poly(ethylene oxide)-block-polyglycidol: synthesis and swelling properties, React. Funct. Polym., 42 (1999) 31-36. DOI: 10.1016/S1381-5148(98)00060-1

[26] J. Herzberger, K. Niederer, H. Pohlit, J. Seiwert, M. Worm, F.R. Wurm, H. Frey, Polymerization of Ethylene Oxide, Propylene Oxide, and Other Alkylene Oxides: Synthesis,

Novel Polymer Architectures, and Bioconjugation, Chem. Rev., 116 (2016) 2170-2243. doi: 10.1021/acs.chemrev.5b00441

[27] M. Liang, C. Niancao, Z. Kun, C. Yuanwei, L. Xianglin, Copolymer of star poly(epsilon-caprolactone) and polyglycidols as potential carriers for hydrophobic drugs, Polym. Adv. Technol., 23 (2012) 748-755. https://doi.org/10.1002/pat.1952

[28] W. Walach, B. Trzebicka, J. Justynska, A. Dworak, High molecular arborescent polyoxyethylene with hydroxyl containing shell, Polymer, 45 (2004) 1755-1762. doi:10.1016/j.polymer.2004.01.033

[29] P. Bharathi, J. S. Moore, Controlled Synthesis of Hyperbranched Polymers by Slow Monomer Addition to a Core, Macromolecules, 33 (2000) 3212-3218. https://pubs.acs.org/doi/abs/10.1021/ma992027c

[30] B. Emilie, G. M. Alejandra, K. Holger, F. Holger, Linear-Hyperbranched Amphiphilic AB Diblock Copolymers Based on Polystyrene and Hyperbranched Polyglycerol, Macromol. Rapid Commun., 26 (2005) 862-867. https://doi.org/10.1002/marc.200500184

[31] D. Wilms, S.-E. Stiriba, H. Frey, Hyperbranched Polyglycerols: From the Controlled Synthesis of Biocompatible Polyether Polyols to Multipurpose Applications, Acc. Chem. Res., 43 (2010) 129-141. doi: 10.1021/ar900158p.

[32] Y. Zhenhua, S. Rui, S. Deyan, Study of multiple melting behaviour of syndiotactic polystyrene in β-crystalline form, Polym. Int., 49 (2000) 1377-1382. https://doi.org/10.1002/1097-0126(200011)49:11<1377::AID-PI497>3.0.CO;2-S

[33] R. Klein, C. Schüll, E. Berger-Nicoletti, M. Haubs, K. Kurz, H. Frey, ABA Triblock Copolymers Based on Linear Poly(oxymethylene) and Hyperbranched Poly(glycerol):

Combining Polyacetals and Polyethers, Macromolecules, 46 (2013) 8845-8852. https://pubs.acs.org/doi/abs/10.1021/ma4015565

[34] J. L. Atkinson, S. Vyazovkin, Thermal Properties and Degradation Behavior of Linear and Branched Poly(L-lactide)s and Poly(L-lactide-co-glycolide)s, Macromol. Chem. Phys, 213 (2012) 924-936. https://doi.org/10.1002/macp.201100681

[35] S. Halacheva, S. Rangelov, V.M. Garamus, Structure and Interactions in Large Compound Particles Formed by Polyglycidol-Based Analogues to Pluronic Copolymers in Aqueous Solution, Macromolecules, 40 (2007) 8015-8021.https://pubs.acs.org/doi/abs/10.1021/ma071151q

[36] P. Bakardzhiev, S. Rangelov, B. Trzebicka, D. Momekova, G. Lalev, V.M. Garamus, Nanostructures by self-assembly of polyglycidol-derivatized lipids, RSC Adv., 4 (2014) 37208-37219. DOI: 10.1039/C4RA03102D

[37] K. K. Bansal, J. Gupta, A. Rosling, J. M. Rosenholm, Renewable poly(δ-decalactone) based block copolymer micelles as drug delivery vehicle: in vitro and in vivo evaluation, Saudi Pharm. J., 26 (2018) 358-368. https://doi.org/10.1016/j.jsps.2018.01.006

[38] Q. Cui, F. Wu, E. Wang, Thermosensitive Behavior of Poly(ethylene Glycol)-Based Block Copolymer (PEG-b-PADMO) Controlled via Self-Assembled Microstructure, J. Phys. Chem. B, 115 (2011) 5913-5922. DOI: 10.1021/jp200659u

[39] Y. Lu, K. Zhou, Y. Ding, G. Zhang, C. Wuac, Origin of hysteresis observed in association and dissociation of polymer chains in water. Phys. Chem. Chem. Phys. 12, (2010), 3188-3194, DOI: 10.1039/B918969F

[40] A. Miasnikova, A. Laschewsky, Influencing the phase transition temperature of poly(methoxy diethylene glycol acrylate) by molar mass, end groups, and polymer architecture, . Polym. Sci. A: Polym. Chem, 50 (2012) 3313-3323. DOI: 10.1002/pola.26116

[41] O. Glatter, A new method for the evaluation of small-angle scattering data, J. Appl. Crystallogr, 10 (1977) 415-421. https://doi.org/10.1107/S0021889877013879

[42] J. S. Pedersen, Analysis of small-angle scattering data from colloids and polymer solutions: modeling and least-squares fitting, Adv. Colloid Interface Sci, 70 (1997) 171-210. https://doi.org/10.1016/S0001-8686(97)00312-6

[43] D. Svergun, Determination of the regularization parameter in indirect-transform methods using perceptual criteria, J. Appl. Crystallogr., 25 (1992) 495-503. DOI: 10.1107/S0021889892001663

[44] S. Manet, J. Schmitt, M. Impéror-Clerc, V. Zholobenko, D. Durand, C.L.P. Oliveira, J.S. Pedersen, C. Gervais, N. Baccile, F. Babonneau, I. Grillo, F. Meneau, C. Rochas, Kinetics of the Formation of 2D-Hexagonal Silica Nanostructured Materials by Nonionic Block Copolymer Templating in Solution, J. Phys. Chem. B, 115 (2011) 11330-11344. doi: 10.1021/jp200213k